Bottom/Subbottom Surveying Using a New, Parametric, Sidescan Sonar

Warren T. Wood*, Joseph F. Gettrust*, Mrinal K. Sen**, and James G. Kosalas***

*Naval Research Laboratory
Code 7432
Stennis Space Center, MS, 39529
Email: warren.wood@nrlssc.navy.mil

**University of Texas Institute for Geophysics
8701 MoPac Blvd N.
Austin, TX, 78759
Email: mrinal@utig.ig.utexas.edu

***Aliant Techsystems
Marine Systems West
6500 Harbour Heights Pkwy
Mukilteo, WA, 98275

Abstract

The Naval Research Laboratory (NRL) has developed a dual-frequency, towed, interferometric, sidescan sonar system known as the Subbottom Swath System, which is capable of detecting objects and structures buried below the sea floor. The transducer geometry is that of a conventional interferometer side scan sonar system but with a more powerful (241 dB re 1 μPa @ 1m) source. As a result of this power, S^3 is capable of generating low frequency (500 Hz - 2 kHz) parametric signals (~203 dB re 1 μPa @ 1m for 1600 Hz) that can easily penetrate several meters to tens of meters into the bottom. Data from a test in Puget Sound, WA show evidence of bottom penetration of parametrically generated sound.

1. Introduction

The Subbottom Swath System (S^3), conceived at the Naval Research Laboratory [1] and developed in cooperation with Aliant Techsystems, represents a breakthrough over conventional side scan sonars in that the earth structure and reflectivity within a vertical plane may be measured with a single ping, (Figure 1). This advance to a 2-D image for each ping is analogous to the advance of side scan (1-D per ping) over single transducer depth finders (a single depth estimate per ping). With the S^3 technology, not just the sea floor but the structures hidden beneath it can be mapped many times more efficiently than was previously possible. High resolution single-channel 3-D surveys could be done in a matter of days instead of weeks. Many of the technical problems encountered in this new technology have been overcome and we are able to demonstrate the bottom penetrating capabilities of S^3 in a test area in Puget Sound, WA.

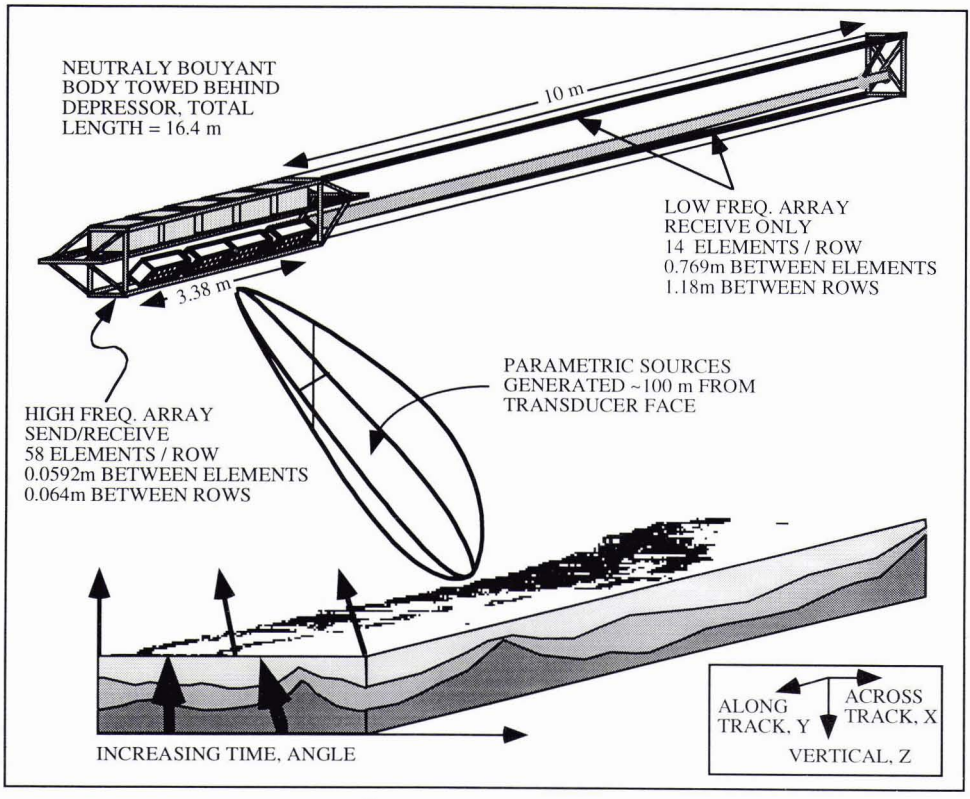

Figure 1. The Subbottom Swath System or S^3 operates using the same geometry as a conventional side scan sonar but with parametrically generated frequencies low enough to penetrate many meters into the seafloor.

2. Theory

In order to maintain high-resolution in the along-track direction with frequencies low enough to penetrate 10's of m, S^3 uses the nonlinear characteristics of high power sound generation, or parametrically generated sound. Through this phenomenon, energy can be transferred from high frequencies with their characteristic beam pattern to much lower frequencies within the same beam. The phenomenon of parametric sound generation was first described mathematically in detail by Westervelt [2,3,4] and is reviewed more succinctly by Clay and Medwin [5], so only a brief overview is given here.

Consider the pressure, (p) at a point, (x_o) on the x axis due to a single frequency, (w_1) plane wave traveling along the x axis with peak amplitude P_o. Assuming, without loss of generality, that we choose time, t=0 to coincide with x_o lying on a wave crest,

$$p(x_o,t) = P_o \cos \omega_1 t \tag{1}$$

The pressure due to a second wave with the same phase and amplitude but different frequency (w_2) can be represented by;

$$p(x_o,t) = P_o \cos \omega_2 t \tag{2}$$

If P_o is large enough that the medium of propagation, (water) behaves anelastically then the total pressure from the two waves at x_o is given not simply by the sum but by;

$$p(x_o,t) = P_o[\cos \omega_1 t + \cos \omega_2 t + m \cos \omega_1 t \cos \omega_2 t] \tag{3}$$

where $m = m(P_0)$ which is a measure of the non-linearity of the system and is quite small (~-40 dB) even at the rather high powers used by S^3. Because

$$2 \cos a \cos b = \cos(a+b) + \cos(a-b) \tag{4}$$

we get

$$p(x_o,t) = P_o[\ \cos \omega_1 t + \cos \omega_2 t + (m/2)\cos \omega_s t + (m/2)\cos \omega_d t\ ] \tag{5}$$

where $\omega_s = \omega_1 + \omega_2$ and $\omega_d = \omega_1 - \omega_2$. This interaction results in 4 waves, of frequencies ω_1, ω_2, ω_s, and ω_d. Thus a source of 11 and 12 kHz would result in parametric conversions to 1 and 23 kHz.

In practice, however, the parametric sound from S^3 is generated by a modulated single frequency rather than interfering dual frequencies. For the field data shown here the two rows of 11.5 kHz transducers are fired simultaneously, but in bursts of 4 cycles on and 3 cycles off for a total of 231 cycles or 20.09 ms resulting in a ω_d of 1.6 kHz. This modulation can be altered to yield a lower ω_d at a cost of decreasing m and signal level, or to yield a higher ω_d at a cost of decreased sediment penetration. The modulation could also be swept resulting in a larger bandwidth for ω_d and therefore increased spatial resolution.

As mentioned above, the parametric sound generation occurs only in the presence of the source frequency and therefore has the same beam pattern, (Figure 2). We are thus able to generate the 1.6 kHz signal with a much narrower along-track beam width and corresponding higher resolution than could be achieved by generating the low frequency signal directly. This is discussed further in the next section.

3. Instrumentation and Operation

Figure 1 is a drawing of the system, (not to scale with the beam or seafloor), built for NRL by Aliant Techsystems [6]. The neutraly buoyant 16.4 m long system is towed at the desired depth behind a depressor. The high frequency (HF) source array is made up of two rows of 11.5 kHz nominal resonance ceramic transducers, 3.38 m long. The electronics for the 58 transducer elements in each row are connected in parallel resulting in a two channel system. The physical separation between elements in each row is 0.0592 m, and the separation between rows, (channels) is 0.064 m. When fired simultaneously the two rows form a very intense beam (20 kW, corresponding to a sound intensity level of 241 dB re 1 µPa @ 1 m), which is relatively wide across-track and relatively narrow along-track, (~60° and 2.5° respectively, down to the -6 dB point, see Figure 2). This allows for high along-track resolution, yet broad across-track coverage maximizing the range ensonified.

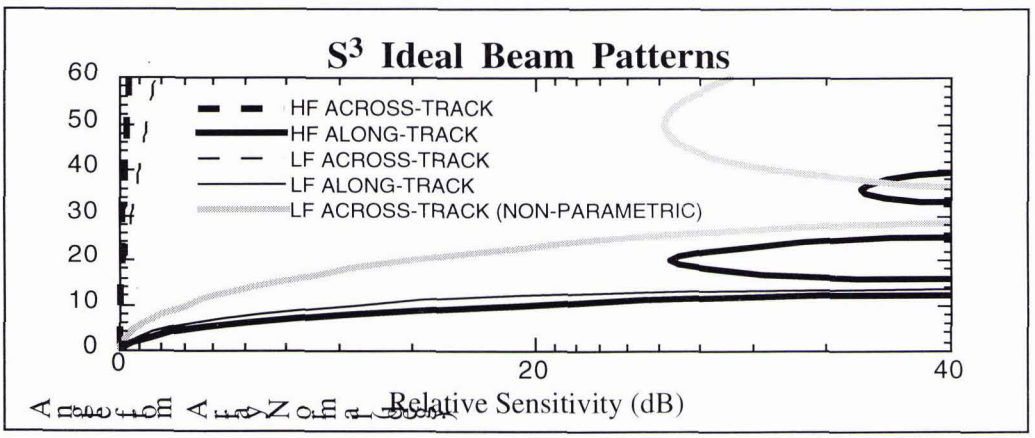

Figure 2. Like a conventional side scan system, the beam pattern is very wide across-track and very narrow along-track. The combined transmit-receive pattern for the along-track LF signal is much narrower (fine curve) than would be possible for the same array under non-parametric conditions, (gray curve), due to the virtual sources lying only within the narrowest part of the HF beam, (heavy black curve). The beams shown here were computed for point sources and receivers and do not include effects of the transducer housing.

The HF source array also acts as a receive array, further narrowing the beam width of the recorded signal and generating a conventional, although very high power, side scan image. As with conventional side scan there is a trade off between the area investigated (maximized with the shallowest towing) and the resolution achieved, (maximized with the deepest towing). Because of the high power used, the system must be towed deeper than ~10 m to prevent transducer cavitation. Also, the parametric sound generation occurs about 100 m from the face of the HF array [5].

As operated during the Puget Sound test, the high-power HF array produced a parametric source at a frequency of 1.6429 kHz with an estimated power level of 204.5 dB (re 1 μPa @ 1 m). The backscattered sound is received by a low frequency, (LF) array located along a "stinger" or "tail" boom, (Figure 1). The 14 hydrophones per row, (element separation 0.769 m and row separation 1.18 m) which make up the two row, 10 m long, LF array are spaced proportionately to give approximately the same beam pattern and direction as the HF array. Figure 2 shows the beam patterns of both arrays. These are combined transmit and receive beams. For the HF array the transmit is the same as the receive beam so the result is just the square of the transmit beam, (heavy and heavy dashed lines). For the low frequency array we assume the LF transmit beam is the same as the HF transmit beam without the side lobes [5]. This is multiplied by the receive beam pattern of the LF array itself to give the LF result shown in Figure 2, (fine and fine dashed lines). The heavy gray line shows what the along-track beam width would be for a 1.6 kHz source generated non-parametrically with an array configured like the LF array. The parametric approach allows for a narrower beam and therefore greater resolution for an array of a given size, making practical a 1.6 kHz system with the along-track resolution comparable to that of a 11.5 kHz system.

4. The Data

The data presented here are from a test cruise in Puget Sound, near Seattle, WA, (water depth <200 m), in which the first clearly identifiable low-frequency returns from the system were recorded, (Figure 3). The data are recorded as four complex time series of 5000 samples each corresponding to each of the two rows of high and low frequency elements. Each time series is digitized after a base band shift, also called heterodyning, or in phase and quadrature down conversion, a process which shifts the band to a lower frequency which then allows the data to be adequately sampled at a rate of 5 kHz. The high frequency data were shifted to DC as is the usual practice, but because the lower frequency is variable they were shifted by 1.3068 kHz. The S^3 was fired once per second and the towing speed was 1.4 kts resulting in 0.72 m/ping. Each ping shown in Figure 3 is simply the sum of the complex absolute values of the two complex samples at each time, after appropriate bandpass filtering.

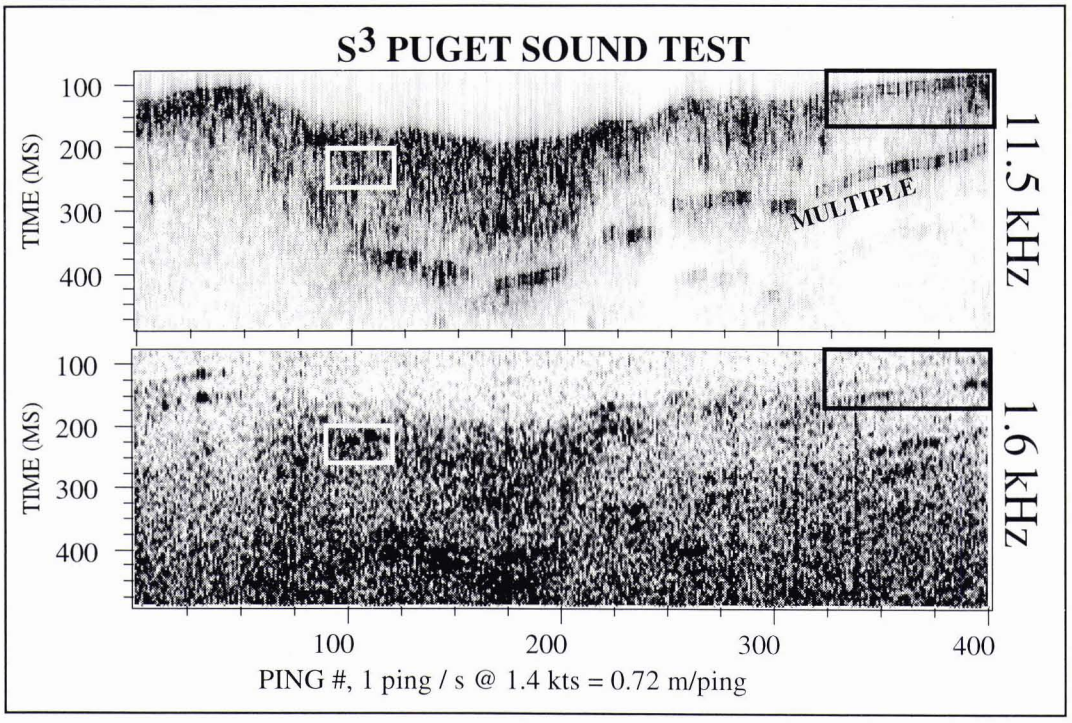

Figure 3. The HF (upper) and LF (lower) scattered returns are largely similar as would be expected but differ significantly in certain locations (boxes) due to bottom penetration. Note the significantly lower signal to noise ratio of the LF data.

5. Data Imaging and Inversion

Processing of the S^3 HF data is virtually identical to the processing of side scan data, but the steps involved with mapping the parametric energy to its proper spatial location involve somewhat different steps. The 4 complex time series are first band pass filtered and also cepstral filtered according to their respective bands to remove events which are known to be noise. At this stage the data are mapped from time and amplitude into the spatial cylindrical coordinates y,R,θ, where R is the range from the ship track, y is measured along the towing track, and θ is the angle from vertical. The complex data at each time are first converted from Cartesian (r,i), to polar (A,ϕ), via

$$A = \text{sqrt}(z_r^2 + z_i^2) \quad \text{and} \quad \phi = \text{atan}\,(z_r\, z_i^* / A) \tag{6}$$

Where * denotes complex conjugate and f is the relative phase angle (electrical angle) between the signals from the upper and lower components of each array. Knowing the distance between the array elements, the angle the array makes with the vertical, and the speed of sound in water allow us to convert this phase angle into a physical angle (θ) measured from the vertical. The range, R is also easily computed giving us the point in image space (R,θ) to which the amplitude at that sample should be mapped. This is different than conventional processing in that the LF data are not forced to lie along a surface but may be mapped to any depth along the circular trajectory given by R.

A more sophisticated imaging (positioning, migration) scheme has been developed which includes a variable velocity function in the sediments and therefore a non circular trajectory [7]. The algorithm is a modification of Kirchoff migration algorithm commonly used in the oil exploration industry [8]. The S^3 data can be viewed as stacked (or coincident source-receiver) data, and a slightly modified Kirchoff post stack migration algorithm is well suited for imaging these data. Our approach involves tracing rays from the source/receiver location to each point in a 2-D velocity model. The travel time and arrival angle for the ray at each grid point in the subsurface are stored in a table, for use as the imaging condition for the S^3 data. The measured amplitude at a given time is mapped via the phase and stored table information to the subsurface location where it originated, assuming that the velocity function is known. This migration algorithm can be modified to include iterative velocity refinement and inclusion of shear wave paths through the sediments in the ray calculation.

A synthetic experiment was conducted to test the inversion algorithm with the results displayed in Figure 4. The model earth was composed of two, semi-parallel rough layers. In the ideal case of no noise (Figure 4, left), the inversion is robust, clearly positioning the backscattered energy on the two rough surfaces. Note, however, that the performance suffers in the presence of noise, (Figure 4, right). This is not so much a characteristic of the inversion algorithm as it is a characteristic of the wavelength, array size, and range. Like conventional side scan systems this one is much more sensitive to errors in phase than errors in amplitude. A signal to noise ratio of 20 dB, which is suitable for most imaging, degrades the migrated image such that the two layers can be seen but little interpretation can be done.

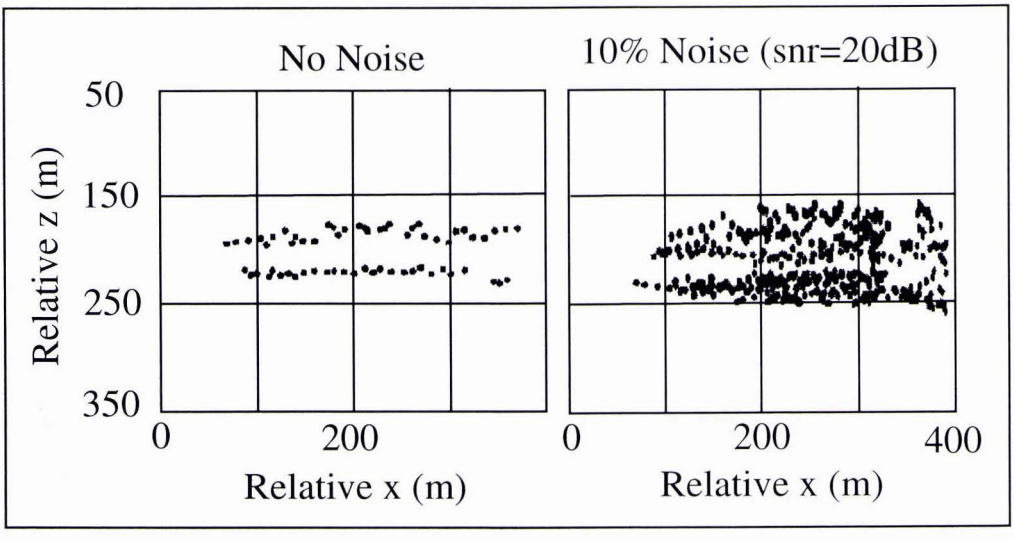

Figure 4. The Kirchoff inversion was applied to a synthetic using an earth model composed of two flat, but rough layers. A signal to noise ratio of better than 20 dB is required for robust performance of the algorithm, [7].

This sensitivity of the inversion due to the presence of noise in phase measurements was seen in the field data as well. While the amplitudes of the events seen in the boxes in Figure 3, (lower) can be seen through the noise, even small amounts of noise in the phase produce large distortions, preventing these data from yielding a satisfactory sub-bottom image. Compounding the problem for this particular data set is the fact that the LF data are aliased, the array elements are > 0.5 wavelengths apart. This is not an insurmountable problem since the less noisy HF data can be used to determine the bathymetry which can then be used to guide the LF inversion. We assume that arrivals at similar times come from similar angles, a reasonable assumption if penetration is not too deep. This divides the LF data into time zones or lanes within which the LF electrical angle varies from $-\pi$ to π. However, it is the noise contamination in the phase measurement which is the main obstacle to creating a subbottom imagewith these particular data.

6. Conclusions

The data image in Figure 3 show strong returns from both high and low frequency signals. Although the signal to noise ratio of the low-frequency data is disappointing, the data clearly show features which are not visible in the corresponding conventional 11.5 kHz image. We interpret these signals as evidence of subbottom penetration. Additional tests have confirmed that the self-noise of the low-frequency array is the limiting factor in the performance of this system [9]. That array is currently being modified to improve its noise characteristics, and additional tests are scheduled for summer 1997.

This work was supported by ONR program element 0601153N31.

References

[1] J. F. Gettrust and M. M. Rowe, "High-resolution geoacoustic studies in deep ocean environments",in *Proceedings of Oceans '91, IEEE* , pp.442-445, 1991.

[2] P. J. Westervelt "Scattering of Sound by Sound" *The Journal of the Acoustical Society of America,* vol. 29, pp.199-203, February 1957.

[3] P. J. Westervelt "Scattering of Sound by Sound" *The Journal of the Acoustical Society of America,* vol. 29, pp.934-935, August 1957.

[4] P. J. Westervelt "Parametric Accoustic Array" *The Journal of the Acoustical Society of America,* vol. 35, pp.535-537, April 1963.

[5] C. S. Clay and H. Medwin, Acoustical Oceanography, New York, John Wiley and Sons, pp. 162-175, 1977.

[6] Aliant Techsystems Marine Systems *SeaMARC 12/1.5 3-D Imager Field Service Manual*, 1992.

[7] M. K. Sen, F. A. Akbar, P.L. Stoffa, and J. F. Gettrust, Imaging of Ocean Subbottom Structure using Swath Mapping Data: Feasability Studies, abstract., *The Journal of the Acoustical Society of America*, vol. 93, p. 2341, 1993.

[8] O. Yilmaz, Seismic data processing, Society of Exploration Geophysicists, Investigations in Geophysics Vol. 2, 1988.

[9] M. T. Kalcic and A. B. Martinez, Subbottom Swath Sonar: SNR Analysis, Naval Research Laboratory Report, NRL/MR/7441--96-8035, December 1996.